



<b>Publication Year</b>	2019
<b>Acceptance in OA</b>	2020-12-23T08:05:48Z
<b>Title</b>	Operational Challenges of the Multibeam Radar Sensor BIRALES for Space Surveillance
<b>Authors</b>	PUPILLO, Giuseppe, BIANCHI, GERMANO, MATTANA, Andrea, NALDI, Giovanni, BORTOLOTTI, CLAUDIO, ROMA, MAURO, SCHIAFFINO, MARCO, PERINI, FEDERICO, LAMA , LUCA, Losacco, Matteo, Massari, Mauro, Di Lizia, Pierluigi, Magro, Alessio, Cutajar, Denis, Borg, Josef, MACCAFERRI, ANDREA, RUSTICELLI, SIMONE, Purpura, Giovanni
<b>Handle</b>	<a href="http://hdl.handle.net/20.500.12386/29129">http://hdl.handle.net/20.500.12386/29129</a>

# Operational Challenges of the Multibeam Radar Sensor BIRALES for Space Surveillance

**Giuseppe Pupillo<sup>(1)</sup>, Germano Bianchi<sup>(1)</sup>, Andrea Mattana<sup>(1)</sup>, Giovanni Naldi<sup>(1)</sup>, Claudio Bortolotti<sup>(1)</sup>, Mauro Roma<sup>(1)</sup>, Marco Schiaffino<sup>(1)</sup>, Federico Perini<sup>(1)</sup>, Luca Lama<sup>(1)</sup>, Matteo Losacco<sup>(2)</sup>, Mauro Massari<sup>(2)</sup>, Pierluigi Di Lizia<sup>(2)</sup>, Alessio Magro<sup>(3)</sup>, Denis Cutajar<sup>(3)</sup>, Josef Borg<sup>(3)</sup>, Andrea Maccaferri<sup>(1)</sup>, Simone Rusticelli<sup>(1)</sup> and Giovanni Purpura<sup>(2)</sup>**

<sup>(1)</sup> National Institute for Astrophysics - Institute of Radio Astronomy (INAF-IRA),  
Via Piero Gobetti 101, 40129 Bologna, Italy, {g.bianchi, g.pupillo, mattana, g.naldi, c.bortolotti, m.roma,  
m.schiaffino, f.perini, l.lama}@ira.inaf.it

<sup>(2)</sup> Politecnico di Milano, Via La Masa 34, 20156 Milano, Italy, {matteo.losacco, pierluigi.dilizia,  
mauro.massari}@polimi.it

<sup>(3)</sup> University of Malta, Msida, MSD 2080, Malta, {alessio.magro, denis.cutajar, josef.borg}@um.edu.mt

## ABSTRACT

This paper illustrates the Italian Bi-static Radar for LEO Survey (BIRALES) sensor for Space Surveillance and Tracking in the LEO regime. BIRALES is a bistatic radar whose receiving part has been refurbished to synthesize up to 32 simultaneous beams in the antenna field of view. The multibeam configuration offers the possibility of estimating the track of the detected objects inside the receiver field of view by analysing the beams illumination sequence. The estimated track is then coupled with the available Doppler shift and slant range measurements. The availability of such a plethora of information is then exploited to perform initial orbit determination with a single passage of a resident space object inside the sensor field of view. This work describes BIRALES sensor setup and operation, showing the performance of the sensor in terms of observation and state estimation capabilities.

## 1 INTRODUCTION

Space debris population is growing and it is recognized as one of the main threats for satellites orbiting around Earth. Therefore, monitoring the space debris environment has become a key issue in the context of all space activities. An international effort is being devoted to improving the performance of optical and radar sensors for space objects monitoring. Collision risk assessment is performed daily by satellite operators who are provided with conjunction data messages to support decisions on the execution of collision avoidance manoeuvres [1]. In addition, re-entry predictions of objects are regularly produced to estimate on ground risks [2]. Both collision risk assessment and re-entry predictions rely on the accurate estimation and prediction of the state of the orbiting objects, which are derived from the tracking of the space objects using dedicated optical, radar and laser sensors. Within this context, this work presents an assessment of the results that are currently being achieved with the Italian Bi-static Radar for LEO Survey (BIRALES) sensor [3].

BIRALES sensor has been developed in the frame of the European Space Surveillance and Tracking (SST) Support Framework. The transmitting part of BIRALES is located in Sardinia (Italy) and it consists of a 7 m in diameter fully steerable dish equipped with a UHF transmitter able to radiate continuous wave and chirped signals at the same time. The BIRALES receiving part is composed of a fraction of the large Northern Cross radio telescope array located at Medicina (near Bologna, Italy). Currently, BIRALES uses 8 among the 64 parabolic cylindrical reflectors of the North-South arm of the Northern Cross. The cylinders are steerable in elevation only along the local meridian and they are equipped with 4 receivers each. From the 32 raw signals, a dedicated pipeline generates 24 independent beams (multi-beam) covering the BIRALES instantaneous field-of-view (FoV) and performs a real-time detection/measurement of the echo in each beam. Each detected target (space debris, satellite, etc.) passing inside the array FoV produces a given beam illumination sequence. Consequently, together with the classical bistatic range and Doppler shift measurements, we can estimate the object angular path inside the sensor FoV during the passage. The angular path estimation is hindered by the complex gain pattern of the antenna, which feature several lobes for each beam whose gain depends on the sensor elevation. Therefore, a suitable algorithm for track reconstruction has been implemented to solve the resulting ambiguities. After track reconstruction, the estimated angular path is coupled with the measured slant range and Doppler shift profiles to perform an initial orbit determination (IOD). It

is worth noting that, thanks to the huge amount of information generated BIRALES, it is possible to perform IOD with a single passage of an object inside the sensor FoV.

The paper is organized as follows. Section 2 provides a detailed description of BIRALES sensor and the issues related to its peculiar gain pattern. Section 3 is devoted to illustrating the initial orbit determination algorithm that currently runs on BIRALES data. Section 4 reports BIRALES performance assessment using both numerical simulations and real data analysis.

## 2 BIRALES Sensor

BIRALES is a bistatic radar composed of two distinct antennas, a receiving and a transmitting one with a baseline of about 580 km. The transmitting antenna is the Radio Frequency Transmitter (RFT) of the Italian Joint Test Range of Salto di Quirra (PISQ) in Sardinia, Italy (see Fig. 1). It consists of a powerful amplifier able to supply a maximum power of 10 kW in the bandwidth 410-415 MHz. It is a 7 m dish completely steerable at a maximum speed of 3 deg/sec and with right hand circular polarization. It is available for operation 24 h/day. Its field of view (FoV) matches almost perfectly the receiving antenna, with a beam of 6 deg.



Fig. 1. BIRALES Tx and Rx location.

The receiving antenna is a portion of the Northern Cross Radio Telescope (see Fig. 2), which is currently one of the largest UHF-capable antenna in the world, being located at the Medicina Radio Astronomical Station, near Bologna, in Northern Italy. It is owned by the University of Bologna but managed and operated by the National Institute for Astrophysics - Institute of Radio Astronomy (INAF-IRA). The portion dedicated to BIRALES receiving antenna is currently composed of 8 parabolic cylindrical antennas of the N/S branch. Each cylinder has 4 receivers installed in the focal line, for a total of 32 receivers. The total collecting area is about 1400 square meters and it allows to detect small objects with sub-metric RCS (Radar Cross Section) at 1000 km of altitude.



Fig. 2. The Northern Cross radio-telescope.

BIRALES works in survey mode and exploits an innovative concept based on two different systems, working at the same time:

- Multi-beam CW unmodulated;
- Single-beam FMCW.

The first system has the purpose of measuring the Doppler shift and the angular profiles of the target, while the second one performs the slant range measurement. For this reason, the transmitter simultaneously radiates a CW (Continuous Wave) unmodulated signal centered at 410.085 MHz and a FMCW (Frequency Modulate Continuous Wave) saw-tooth chirped signal with about 4 MHz bandwidth centered at 412.5 MHz. BIRALES utilizes two different receiving chains for these two kind of signals: the echoes from the unmodulated CW are sent to a digital backend able to generate the multi-beam configuration inside the antenna FoV, whereas the chirped signals are combined into an analogue beamformer before being processed by the ranging measurement module (see Fig. 3).

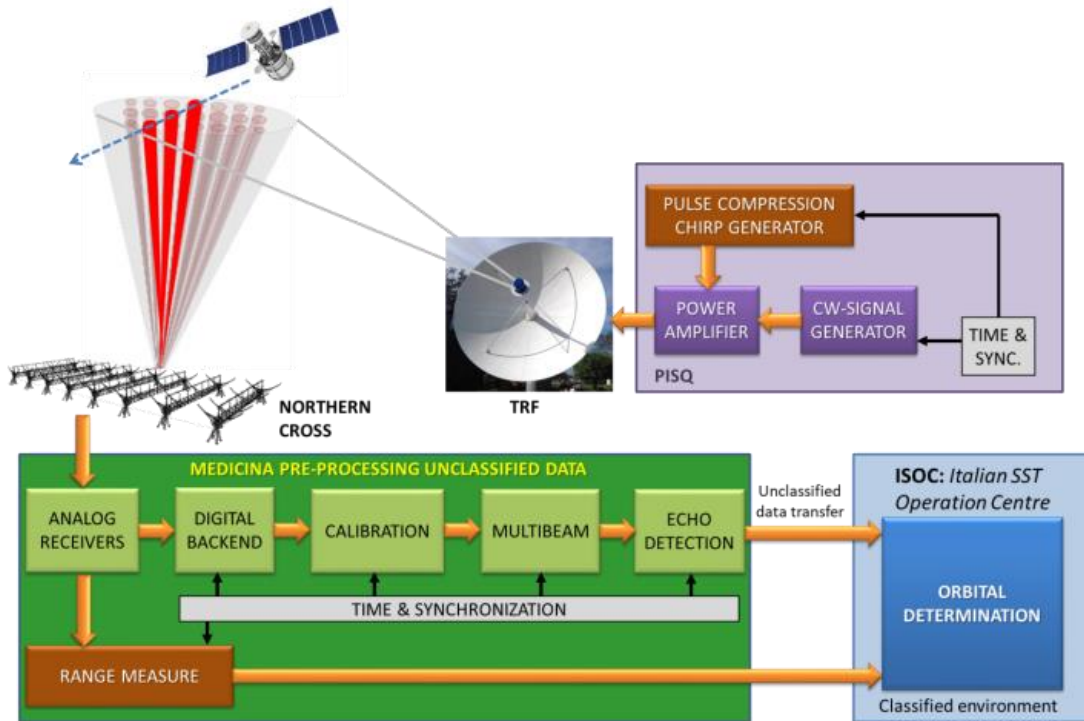


Fig. 3. BIRALES system architecture.

## 2.1 BIRALES gain pattern

Due to the large number of receivers installed on the Northern Cross, BIRALES FoV can be populated with many independent beams. When an object transits inside the antenna FoV, the beams are illuminated by the reflected radio waves. Thus, by looking at the beam illumination sequence, it is possible to estimate the angular path of the transiting object, with a higher level of details with respect to a single-beam system. The information about the sequence of illuminated beams allows to discern the trajectory of the object. In parallel, the RFT emits also a chirp of known period and span, in order to estimate the range; in this way, BIRALES acquires all the information to estimate the target's orbit with a ranging error below 100 m.

Figure 4 shows the distribution of the beams in the RX FoV. The angles  $\Delta\gamma_1$  and  $\Delta\gamma_2$  are the angular deviations with respect to the RX pointing direction. The task of estimating the angular path of the transiting object is complicated by the geometry of the receiving array, which is responsible for the generation of a complicated gain pattern mask, where each beam is characterised by a main lobe, side lobes, and several "grating lobes" in both  $\Delta\gamma_1$  and  $\Delta\gamma_2$  directions.

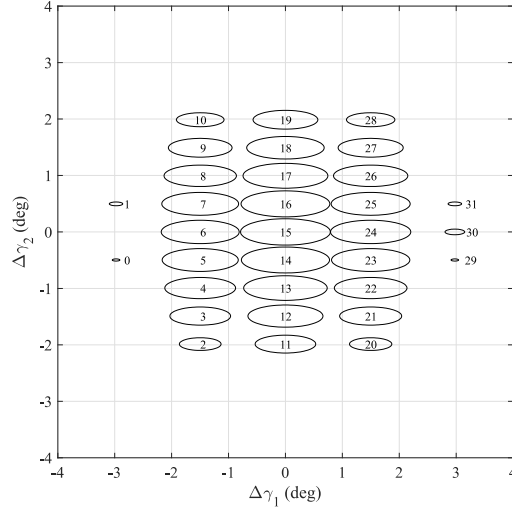


Fig. 4. BIRALES 32-beam receiver configuration. The angles  $\Delta\gamma_1$  and  $\Delta\gamma_2$  are the angular deviations with respect to the receiver pointing direction in the sensor reference frame.

Grating lobes are exact copies of the beam main lobe which regularly appear in both angular directions. The gain of these grating lobes may be more or less significant according to the investigated beam. The gain pattern of each single beam mainly depends on its position inside the receiver FoV. Beams located close to the boresight of the sensor typically show only a main lobe and side lobes, whose gain is much lower than the one of the main lobe. An example is given in Figure 5a for beam 24, with one main gain peak and other secondary, much weaker, side lobes. These beams will be defined throughout the paper as dominant beams. On the contrary, beams located at the boundaries of the FoV typically have the main lobe and one grating lobe, whose gain is comparable with the one of the main lobe. Figure 5b shows the gain pattern of beam 30: besides the gain peak associated to the main lobe, the pattern shows another gain peak, whose gain is comparable with the one of the main lobe. When all the 32 beams are considered, the combination of main lobes and grating lobes creates a complex configuration. As a consequence, when an object transits inside the RX FoV, both main lobes and grating lobes are responsible for the generation of the SNR profiles of the multibeam system, and the beam illumination sequence does not automatically define a single trajectory. Thus, a dedicated algorithm for identifying the correct path of the object is required.

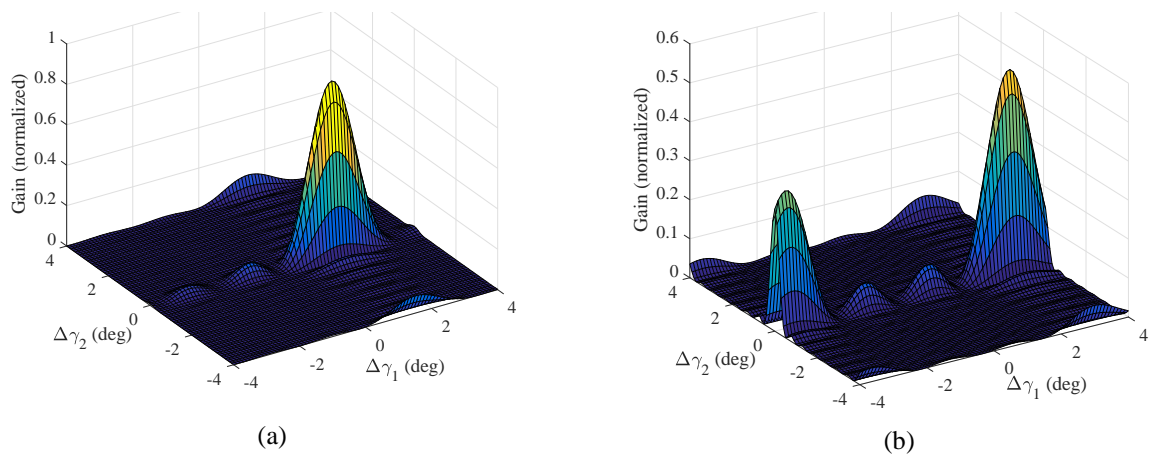


Figure 5: Example of gain patterns for single beams. (a): beam 24, with one main lobe and several minor side lobes; (b): beam 30, with one main lobe, one grating lobe and minor side lobes.

### 3 INITIAL ORBIT DETERMINATION ALGORITHM

The starting point for the IOD algorithm implemented for BIRALES sensor is represented by a measurement text file including, for all the beams illuminated during the object passage, the epoch and the recorded slant range, Doppler shift and SNR measurements. Then, the algorithm is divided in two parts:

- *Track reconstruction*: this part is dedicated to the estimation of the track of the object inside the receiver FoV starting from the available SNR and slant range measurements;
- *State estimation*: the state of the object is estimated on the basis of the available slant range and Doppler shift measurements, and the estimated track.

In the following sections, both phases are described in detail. The analyses are performed considering the current configuration (32 beams) and slant range measurements available.

#### 3.1 Track reconstruction

The peculiar gain pattern of BIRALES receiver affects the approach to be followed for the definition of the object track inside the receiver FoV. The idea at the basis of the approach is to reconstruct the track of the object by looking at the sequence of illumination of the beams. This, in turn, essentially consists in matching the measured SNR profile with the one obtained by the estimated track. The algorithm can be divided in two phases:

- a first *phase S1*, in which a first estimate for the object track is obtained by looking at the recorded SNR peaks;
- a second *phase S2*, in which the obtained track is used as a first guess for a least-squares fit aimed at minimizing the residuals with respect to the whole SNR profile of all the illuminated beams.

The first estimate in phase S1 is obtained by looking at all the SNR peaks recorded during the passage of the object and associating each signal peak to a given gain peak of a specific beam. This probably represents the most challenging aspect of the track definition algorithm, given the presence of multiple gain peaks per beam. When one beam is illuminated, indeed, it is not straightforward to understand which gain peak is responsible for the beam illumination. It is therefore necessary to identify some SNR peaks that are likely to be associated to specific gain peaks. The idea behind the implemented approach consists in starting the process by considering the largest SNR peak recorded by each dominant beam. When one of these beams is illuminated, its maximum signal peak is automatically associated to the main lobe of the beam in terms of angular deviation. By assuming a linear trend in time of the angular deviation profiles  $\Delta\gamma_1$  and  $\Delta\gamma_2$  and performing a first polynomial fit, this allows us to obtain a first estimate of the track of the object inside the receiver FoV. Once this track is defined, all SNR peaks can be considered, including the ones of beams with multiple comparable gain peaks. Each signal peak can then be associated to a specific gain peak by identifying the lobe with minimum deviation with respect to the previously estimated track at the epoch the SNR peak was detected. This procedure provides us with a full list including, for each recorded signal peak, the corresponding time epoch and angular deviations of the associated gain peaks. These data are processed with a new linear fit, and a refined first guess for the object track is obtained.

The described approach allows us to maximize the information extracted from the beam illumination sequence by simply looking at the recorded SNR peaks and exploiting the gain pattern. This procedure does not require any other measurement apart from the SNR. If slant range measurements are also available, then a further step can be performed. Starting from the estimated object track, and assuming a polynomial trend of the angular deviations with time, by knowing the slant range measurements at each observation instant, it is possible to perform a least-squares fit aimed at minimizing the residuals with respect to the whole SNR profile of all the beams. This second step, referred to as S2, grants better accuracy to the estimate and concludes the track definition phase.

#### 3.2 State estimation

The output of the track definition phase is a value of  $\Delta\gamma_1$  and  $\Delta\gamma_2$  for each observation instant. These two estimates, along with the Doppler shift and slant range measurements, are used to estimate the state and covariance of the object at the epoch of the first observation. The estimation is done with a Levenberg-Marquardt least-squares batch algorithm and requires an accurate model for the object dynamics. The considered high-fidelity propagator, called AIDA (Accurate Integrator for Debris Analysis), includes the gravitational model EGM2008 up to order 10, the atmospheric drag with the atmosphere model NRLMSISE-00, third body perturbations, and solar radiation pressure

with a dual-cone model for Earth shadow for objects whose geometrical parameters are known. For unknown objects, only gravitational and third-body effects are considered.

## 4 BIRALES PERFORMANCE

This section is devoted to assessing the performance of BIRALES. More specifically, Section 4.1 provides the results of a statistical analysis performed with numerical tests on a dedicated software simulator. Section 4.2 reports some correlation statistics during BIRALES observation campaigns. Finally, Section 4.3 illustrates the results obtained by processing the real data from the observation of two targets.

### 4.1 Statistical performance on a catalogue of objects

Given a catalogue of space objects, a software simulator has been developed to identify the passages of the objects inside BIRALES FoV and to generate the simulated measurements in terms of slant range, Doppler shift and SNR (see [4] for further details). The simulated measurements are provided as input to the initial orbit determination module. The analysis is performed assuming the following levels of measurement noise: 3 m of standard deviation for the slant range (SR), 9 Hz of discretization for the Doppler shift (DS), and a white Gaussian noise for the SNR, assuming a ratio of 30 dB between the nominal signal and the added white noise.

An observation window of two days is considered, covering the range 5-6 September 2018, with 2490 objects from the NORAD catalogue with at least one passage in the sensor field of view. For all objects, only the first passage is exploited to perform IOD (i.e. the objects are assumed to be unknown). The performance is assessed in terms of mean position and velocity errors ( $\varepsilon_p$  and  $\varepsilon_v$ , respectively), and the associated mean standard deviations  $\sigma_p$  and  $\sigma_v$ . The results are reported in Table 1. The overall number of observable objects is quite low. This is partly due to our decision of selecting the first passage only, and partly to the peculiarity of the sensor of detecting meridian passages only with a narrow field of view. Let us now focus on the IOD performance. As can be seen, if no measurement noise is added to the simulated measurements, the accuracy granted is relatively high, with a mean position error of the order of 1 m. If measurement noise is considered, the performance decreases, with an average decrease in accuracy of around one order of magnitude in position and two orders of magnitude in velocity. Still, the average position error is lower than 100 m.

Noise	# of objects	$\varepsilon_p$ (km)	$\varepsilon_v$ (km/s)	$\sigma_p$ (km)	$\sigma_v$ (km/s)
-	29	1.29e-3	2.07e-4	4.84e-4	3.50e-5
DS and SR	30	7.87e-3	2.91e-3	6.78e-2	5.38e-3
DS, SR and SNR	27	5.39e-2	1.32e-2	7.47e-2	4.38e-3

Table 1: BIRALES IOD statistical performance.

### 4.2 Correlation statistics

BIRALES sensor was recently adopted to perform survey campaigns within the European SST Support Framework. To this aim, a software tool has been developed to correlate the measurements obtained during the observation campaigns with the passage of space objects from the NORAD catalogue. The input to the correlation is the set of measurements generated during a detected passage. The measurements associated to each detection are collected in a Tracking Data Message (TDM) file and processed by the correlator to produce an output TDM file containing filtered data. More specifically, in case of successful correlation, the output TDM reports one measurement for each lobe of the illuminated beams that has been crossed by the object during the passage.

The correlation process is divided in two steps. In the first step, only the measured Doppler profile is checked against the predicted profiles of all the objects from the catalogue to find a match. If the match is successful, the second step starts. For each illuminated beam, the object is propagated using SGP4 to check whether the associated measurement epochs are compatible with the presence of the object in any lobe (main or grating) of the beam. In case of compatible measurements, the lobe of the beam is marked as crossed and is included in the sequence of illuminated lobes, together with its pointing angles. At the end of the correlation process, the resulting sequence is used to generate the output TDM file.

Figure 6 shows some statistical results obtained during an observation campaign conducted in the period September 25, 2019 – October 7, 2019. For each day, the figure reports the percentage of correlated TDMs by adopting only Doppler matching as correlation criterion (orange bar), and by adding beam lobes crossing as additional criterion. More specifically, the blue bars refer to the case of beam lobes crossing checked on the main lobes only, whereas crossing is checked on all lobes to obtain the grey bars. As can be seen, on average, more than 80% of the TDMs generated daily by the sensor are correlated with the passage of NORAD catalogued objects in the sensor FoV.

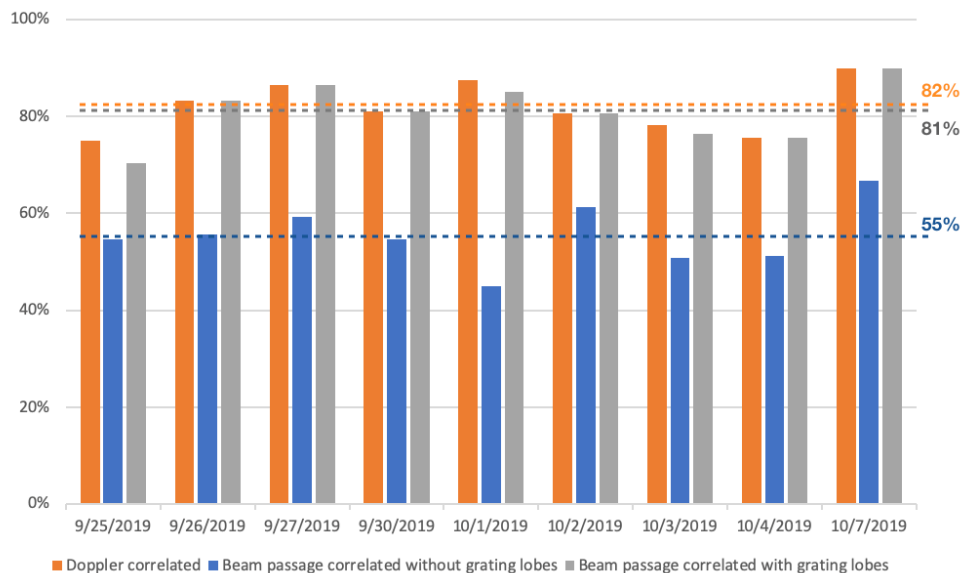


Fig. 6. BIRALES correlation statistics for the observation period September 25, 2019 – October 7, 2019.

### 4.3 Examples of IOD on real data

Two examples of the performance of the IOD algorithm on real data are offered in this section. In the first example BIRALES has been used in tracking mode, i.e. given the target and the predicted epoch of its passage, the pointing angles have been selected to let the object pass at the center of the sensor FoV. The selected target is the rocket body SL-8 R/B (NORAD ID 12792) at its predicted passage on March 5, 2019 (11:02:35.08 UTC). Figure 7a reports the SNR profiles measured by each beam during the passage, which show an “increase-decrease” trend that is typical for observations performed in tracking mode, with beam 15 (the central beam) providing the highest peak. Figure 7b reports the result of the track reconstruction step. The estimated angular path is shown in black and is compared with the same angular path as predicted from the TLE (in blue). The estimated track is then coupled with the Doppler shift and slant range measurements to obtain an estimate of the state of the object at the epoch of the first measurement. Table 2 shows a comparison between the reference state vector as computed from the TLE and the estimated one at the epoch of the first observation. For the case under study, the maximum norm of their difference is 320 m in position and 60 m/s in velocity.

The second example deals with the typical measurements obtained by operating BIRALES in survey mode. The survey was conducted on March 10, 2019 by pointing BIRALES Rx northward to an elevation of 60 deg, whereas BIRALES Tx pointing angles were: azimuth = 9.43 deg and elevation = 34.94 deg. Figure 8a reports the SNR profiles measured at 11:13:56.12 UTC, which have been correlated to the passage of the object with NORAD ID 11788. Unlike the previous example, the overall profile appears to be less regular. This is a consequence of the pointing direction of the sensor. While operating in survey mode, the transiting objects are typically detected at the boundaries of the Rx FoV. As a consequence, the contribution of the grating lobes becomes more relevant. Figure 8b reports the result of the track reconstruction, whereas Table 3 shows a comparison between the reference state vector as computed from the TLE and the estimated one at the epoch of the first observation. For this second example, the maximum norm of their difference is 460 m in position and 35 m/s in velocity.

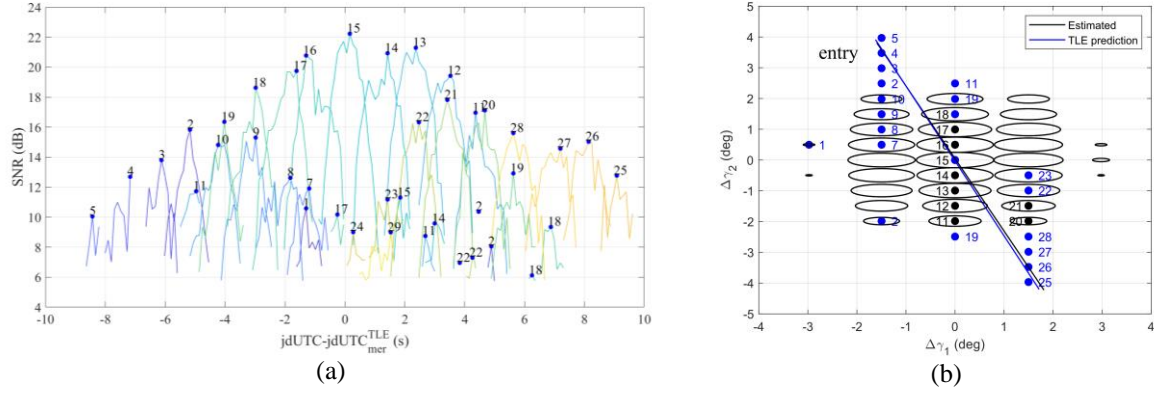


Figure 7: BIRALES IOD algorithm applied to the data measured during the passage of the rocket body SL-8 R/B (NORAD ID 12792) on March 5, 2019 (11:02:35.08 UTC). (a): SNR profiles; (b): estimated angular profile.

	$r_x$ (km)	$r_y$ (km)	$r_z$ (km)	$v_x$ (km/s)	$v_y$ (km/s)	$v_z$ (km/s)
Reference (TLE)	4.62894e3	-1.71229e3	5.15172e3	-3.61731	4.52153	4.73237
Estimate (IOD)	4.62862e3	-1.71237e3	5.15164e3	-3.56555	4.58127	4.71365

Table 2: BIRALES IOD results for the rocket body SL-8 R/B, epoch March 5, 2019 (11:02:35.08 UTC). The reference state vector and the estimate are expressed in ECI reference frame.

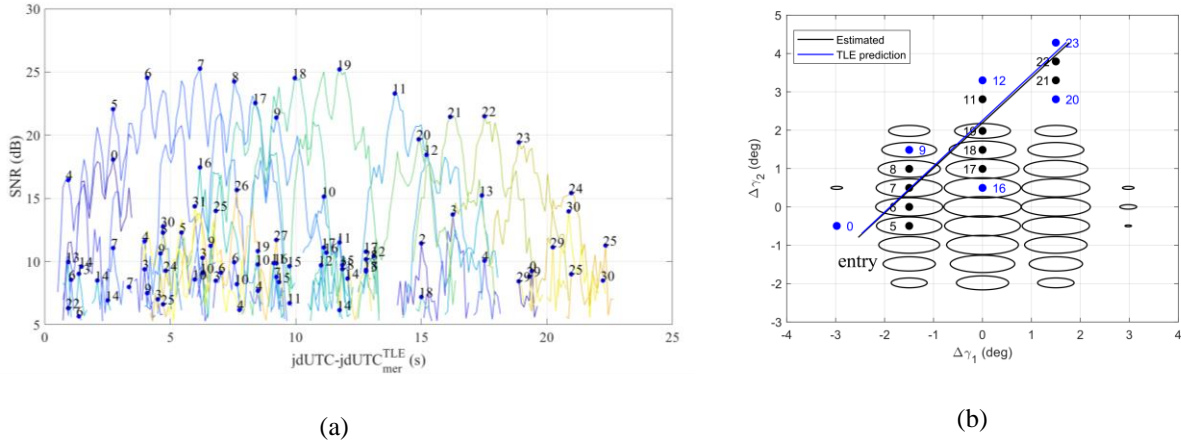


Figure 8: BIRALES IOD algorithm applied to the data measured during the passage of the object with NORAD ID 11788 on March 10, 2019 (11:13:56.12 UTC). (a): SNR profiles; (b): estimated angular profile.

	$r_x$ (km)	$r_y$ (km)	$r_z$ (km)	$v_x$ (km/s)	$v_y$ (km/s)	$v_z$ (km/s)
Reference (TLE)	4.72147e3	-1.07162e3	5.49140e3	5.18646	3.68703	-3.70663
Estimate (IOD)	4.72101e3	-1.07143e3	5.49127e3	5.18173	3.72199	-3.70367

Table 3: BIRALES IOD results for the object with NORAD ID 11788, epoch March 10, 2019 (11:13:56.12 UTC). The reference state vector and the estimate are expressed in ECI reference frame.

## 5 CONCLUSIONS

This paper illustrated the system architecture of the innovative BIRALES sensor, as well as the tailored initial orbit determination algorithm. The performance of the sensor in terms of achievable accuracy of the orbital estimation process has been assessed with numerical simulations. The results show that the data provided by the sensor can be processed to estimate the orbital states with reasonable accuracy with just a single passage of the object inside the field of view of the sensor. Future developments will include experimental testing with slant range measurements, and the possible coupling with other Italian and European sensors.

## ACKNOWLEDGEMENTS

The authors acknowledge the support of the Italian Space Agency and the Italian National Institute for Astrophysics through the grant agreement n. 2015-028-R.O. (Space Debris IADC activities support and SST pre-operative validation). The research activities described in this paper were performed within the European Commission Framework Programme H2020 and Copernicus “SST Space Surveillance and Tracking” contracts No. 785257-2-3SST2016 and No. 237/G/GRO/COPE/16/8935-1SST2016. The Radio Frequency Transmitter is a facility of the Italian Air Force, located at Italian Joint Test Range of Salto di Quirra in Sardinia. The Northern Cross Radio Telescope is a facility of the University of Bologna operated under agreement by the National Institute for Astrophysics - Institute of Radio Astronomy (INAF-IRA).

## REFERENCES

1. K. Merz, B. Bastida Virgili, V. Braun, T. Flohrer, Q. Funke, H. Krag, S. Lemmens, Current collision avoidance service by ESA's Space Debris Office, in "Proceedings of the 7th European Conference on Space Debris", Darmstadt, Germany, 2017.
2. C. Pardini, L. Anselmo. Re-entry predictions of three massive uncontrolled spacecraft, in "Proceeding of the 23rd International Symposium on Space Flight Dynamics", Pasadena, USA, 2012.
3. A. Morselli, P. Di Lizia, G. Bianchi, C. Bortolotti, S. Montebugnoli, G. Naldi, F. Perini, G. Pupillo, M. Roma, M. Schiaffino, A. Mattana, E. Salerno, A. Magro, K. Z. Adami, R. Armellin, A. L. Sergiusti, W. Villadei, F. Dolce, M. Reali, J. Paoli. A new high sensitivity radar sensor for space debris detection and accurate orbit determination, in "Proceeding of Metrology for Aerospace", Benevento, Italy, 2015.
4. M. Losacco, P. Di Lizia, M. Massari, A. Mattana, F. Perini, M. Schiaffino, C. Bortolotti, M. Roma, G. Naldi, G. Pupillo, G. Bianchi, D. Cutajar, A. Magro, C. Portelli, M. Reali, W. Villadei. Orbit determination of resident space objects with the multibeam radar sensor BIRALES, in "Proceeding of the 2018 Space Flight Mechanics Meeting", Kissimmee, USA, 2018.